



Nonlinear optical properties of silicon nanoclusters/nanocrystals doped SiO₂ films: Annealing temperature dependence

Ito, Masahiko
Imakita, Kenji
Fujii, Minoru
Hayashi, Shinji

(Citation)

JOURNAL OF APPLIED PHYSICS, 108(6):63512-63512

(Issue Date)

2010-09-15

(Resource Type)

journal article

(Version)

Version of Record

(URL)

<https://hdl.handle.net/20.500.14094/90001279>



Nonlinear optical properties of silicon nanoclusters/nanocrystals doped SiO₂ films: Annealing temperature dependence

Masahiko Ito, Kenji Imakita, Minoru Fujii,^{a)} and Shinji Hayashi

Department of Electrical and Electronic Engineering, Graduate School of Engineering, Kobe University, Rokkodai, Nada, Kobe 657-8501, Japan

(Received 20 May 2010; accepted 16 July 2010; published online 20 September 2010)

Comprehensive studies on nonlinear refractive indices (n_2) of SiO₂ films containing Si nanocrystals and/or nanoclusters (SiO₂:Si-ncs) are performed. The comparison of the nonlinear refractive indices with the electron spin resonance signals reveals that defect states play a major role in the large n_2 when the annealing temperature is low, i.e., when Si nanoclusters exist in films. On the other hand, when Si nanocrystals are grown by high-temperature annealing, the contribution of defect states becomes small and that of the quantized electronic states of Si nanocrystals becomes large. The present results demonstrate that both the defect states and the quantized electronic states should be taken into account to explain the origin of large n_2 of SiO₂:Si-ncs and to optimize the structure to maximize n_2 . © 2010 American Institute of Physics. [doi:10.1063/1.3480821]

I. INTRODUCTION

Silicon dioxide (SiO₂) films containing silicon (Si) nanocrystals have been attracting great attention as Si-based optoelectronic materials because of the high luminescence efficiency in the visible and near infrared regions and the large nonlinear optical responses.^{1–6} Since they can be prepared by a conventional semiconductor technology such as sputtering,^{6–8} chemical vapor deposition,^{3,5,9} and ion implantation,^{1,2,10} they are considered to be one of the key materials for future silicon-based nonlinear optical devices such as all optical switches and modulators.¹¹

In this material, Si nanocrystals are considered to be responsible for the large nonlinear optical responses. In fact, large nonlinear refractive indices (n_2) have been reported in various forms of Si nanocrystal samples.^{1–6,12–23} An example is porous Si prepared by electrochemical etching of Si wafers.^{12–14} Another one is laser ablated Si nanocrystals deposited on a quartz substrate^{15–17} and dispersed in organic solvents.^{18,19} In the case of SiO₂ films containing Si nanocrystals, large n_2 has been observed irrespective of the preparation procedures, i.e., plasma enhanced chemical vapor deposition,^{3,5} sputtering,⁶ and ion implantation.^{1,2} The reported values of n_2 are much larger than those of bulk Si crystal ($\sim 10^{-14}$ cm²/W) (Refs. 24–26) and SiO₂ ($\sim 10^{-16}$ cm²/W),^{27,28} although they are distributed in a very wide range ($(\sim 10^{-7}) \sim 10^{-13}$ cm²/W).^{1–6}

Because of the large variation in the reported values of n_2 , comparison of experimental data with calculation is not straightforward and thus the origin of large n_2 is not fully elucidated. The most widely believed origin is the quantized electronic states in nanocrystals.^{3–5} The enhancement of n_2 by the quantum size effects has been discussed experimentally and theoretically for a variety of semiconductor nanocrystals.^{29–34} In the case of Si nanocrystals in silica matrices, strong enhancement of n_2 with decreasing the size is predicted theoretically.^{35,36} This has been proved, although

quantitatively, by some experimental studies.^{3,4} Another possible origin of large n_2 is defects in or on the surface of silicon nanocrystals. Vijayalakshmi *et al.*² proposed that surface states contribute to large n_2 of Si nanocrystals. Takagahara and Hanamura³⁷ reported that localization of excitons at disorders or impurities enhances its oscillator strength, and hence the nonlinear optical responses.

One of the purposes of this work is to distinguish the contributions of quantized electronic states and defect states to n_2 of SiO₂ films containing Si nanocrystals and/or nanoclusters. To achieve this purpose, we prepare a large number of samples in wide ranges of preparation parameters and clarify the relation between the preparation parameters and n_2 . For the characterization of samples, we perform electron spin resonance (ESR) and Raman scattering spectroscopy. We show that both defect states and quantized electronic states contribute to n_2 and the relative contributions depend on preparation parameters.

II. EXPERIMENTAL PROCEDURE

In this work, we prepare SiO₂ films containing Si nanocrystals and/or Si nanoclusters by a cosputtering method in wide ranges of preparation parameters. As we discuss later, depending on the preparation parameters, Si nanocrystals or nanoclusters are formed in the films.^{7,8} Hereafter, we denote both types of the samples as SiO₂:Si-ncs.

Si and SiO₂ were simultaneously sputter-deposited in Ar gas on a quartz substrate, and the deposited film (about 12 μ m in thickness) was annealed in a N₂ gas atmosphere for 30 min at temperatures from 600 to 1250 °C. The excess Si concentration was changed from 6 to 22 vol %. The annealing temperature strongly affects the sample morphology.³⁸ In as-deposited samples, very small amorphous Si nanoclusters are dispersed in a film. The number and size of Si nanoclusters increase with increasing the annealing temperature. When the annealing temperature

^{a)}Electronic mail: fujii@eedept.kobe-u.ac.jp.

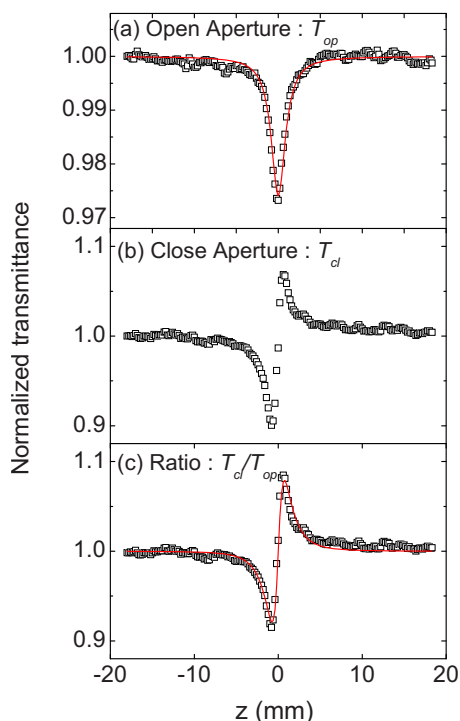


FIG. 1. (Color online) Typical z-scan traces, (a) an open aperture, (b) a close aperture, (c) the ratio, for the sample with the excess Si concentration of 22 vol % and the annealing temperature of 1150 °C. The peak intensity of the incident light is 2.9 GW/cm². Solid curves are the results of the fitting by the z-scan model (Ref. 39).

reaches ~1000 °C, Si nanocrystals start to emerge. The ratio of nanocrystals to nanoclusters increases at higher annealing temperatures.

X-band ESR was measured by a conventional ESR spectrometer (JES-TE300, JEOL) at room temperature. The modulation frequency and amplitude for ESR measurements were 100 kHz and 320 G, respectively. The g value was determined by using the signal from Mn²⁺/MgO powder as a calibration reference. Raman measurements were carried out in a conventional 90° scattering configuration by using a triple monochromator equipped with a charge-coupled device detector. The excitation source was the 488 nm line of an Ar-ion laser.

The nonlinear optical responses [n_2 and two photon absorption coefficient (β)] of SiO₂:Si-ncs were measured by a z-scan method.^{6,39} The excitation source was the mode-locked Ti:sapphire femtosecond laser with the pulse width of 70 fs and the repetition frequency of 82 MHz. The photon energy was varied from 1.52 to 1.66 eV. The incident beam was focused on a sample by a lens with the focal length of 50 mm. The beam waist and diffraction length determined by a knife edge method were 15 μ m and 1 mm, respectively. The peak intensity was lower than 12 GW/cm² to avoid thermal effects.

III. RESULTS AND DISCUSSION

A. Annealing temperature dependence of n_2 and β

Figure 1 shows a typical result of a z-scan measurement; (a) an open aperture (T_{op}), (b) a close aperture (T_{cl}), and (c) the ratio (T_{cl}/T_{op}). Open squares and solid curves represent

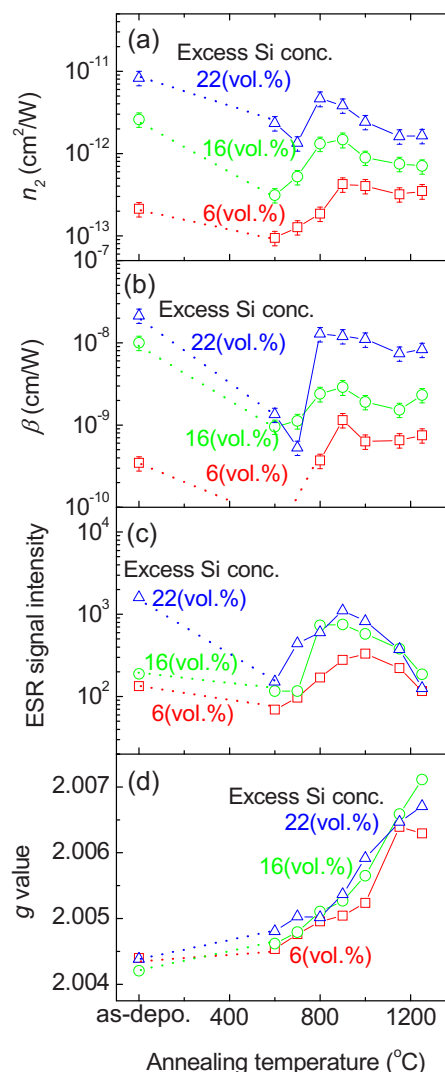


FIG. 2. (Color online) Annealing temperature dependence of (a) n_2 , (b) β , (c) ESR signal intensity, and (d) g value for series of samples with different excess Si concentrations (\square : 6, \circ : 16, \triangle : 22 vol %). In (b), β for the samples with the excess Si concentration of 6 vol % and the annealing temperatures of 600 and 700 °C are not shown because they are below the detection limit.

experimental data and results of fitting by the model commonly used for the analysis of the z-scan measurement, respectively.³⁹ Details of the analysis procedure are shown in our previous papers.^{6,40} The results are well-fitted by the model and thus the n_2 and the β are obtained with high accuracy.

Figures 2(a) and 2(b) show annealing temperature dependence of n_2 and β , respectively, for the samples with three different excess Si concentrations. At almost all annealing temperatures studied, n_2 and β are larger for the samples with larger amount of excess Si. For a fixed excess Si concentration, n_2 exhibits complicated annealing temperature dependence. The dependence is similar for all series of samples with different excess Si concentrations. When the annealing temperature is low (≤ 700 °C), n_2 is smaller than that of as-deposited samples. At higher annealing temperatures, it increases and reaches the maximum at around 800–900 °C, and then decreases. β shows similar annealing temperature dependence. This complicated annealing tem-

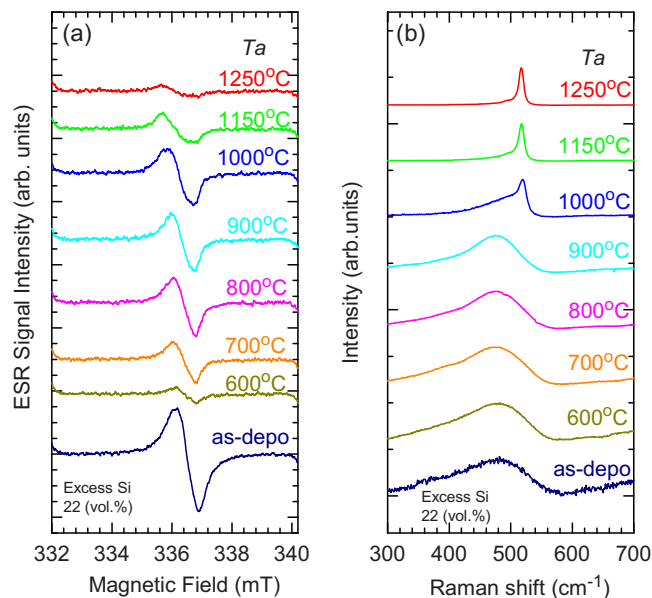


FIG. 3. (Color online) Annealing temperature dependence of (a) ESR spectra and (b) Raman spectra for the samples with the excess Si of 22 vol %.

perature dependence of n_2 strongly suggests that the origin of the large n_2 cannot be explained by a simple quantum confinement model. If only the quantized electronic states are the origin of the large n_2 , n_2 should monotonously decrease with increasing the annealing temperature because of the size increase in Si nanoclusters or nanocrystals.³⁵

As the origin of the large n_2 of SiO_2 :Si-ncs, defect states are also considered.^{2,37} To study the correlation between the defect density and n_2 , we performed ESR measurements. Figure 3(a) shows ESR spectra for the samples with 22 vol % excess Si. We can see that the signal intensity depends strongly on the annealing temperature. Figures 2(c) and 2(d) show annealing temperature dependence of the ESR signal intensity and the g value, respectively. Before discussing the origin of the ESR signals in detail, we roughly compare the annealing temperature dependence of the intensity with that of n_2 . At the first glance, the annealing temperature dependence of the ESR intensity is similar to that of n_2 . This suggests that defects contribute at least partly to the n_2 and β . However, if we closely compare Figs. 2(a) and 2(c), we notice some differences. For example, above 900 °C, the spin density, i.e., ESR signal intensity, decreases much faster than n_2 and β . Furthermore, compared to n_2 and β , spin density does not depend strongly on the excess Si concentration. In Fig. 4, n_2 is plotted as a function of the ESR signal intensity. Although there exists a correlation between these two values, the data are scattered more than one order of magnitude. The large scattering of the data suggests that defects are not an only origin of the large n_2 . We believe that the contribution of the quantized electronic states of Si nanocrystals or nanoclusters in addition to the defect states results in the large scattering of the data.

B. Origin of large n_2 at different annealing temperatures

From the above discussion, it is clear that defects play a significant role in the large n_2 of SiO_2 :Si-ncs. Here, we iden-

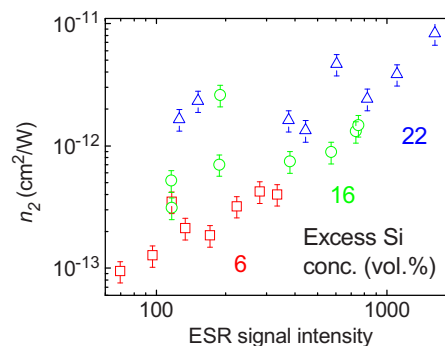


FIG. 4. (Color online) n_2 as a function of ESR signal intensity. The data of all samples, i.e., different excess Si concentrations (\square : 6, \circ : 16, \triangle : 22 vol %) and different annealing temperatures, are plotted.

tify the defects from ESR and Raman data. As shown in Fig. 2(d), the g value gradually increases up to 800 °C and, above this temperature, it increases rapidly. The behavior of the g value suggests the existence of different kinds of defects.⁴¹ The signal with the g value of ~ 2.004 is usually assigned to the defects in SiO_x (EX center),⁴² while that with the g value of ~ 2.006 to dangling-bonds at Si– SiO_2 interfaces (P_b center).⁴³

A comparison of Figs. 2(c) and 2(d) leads us to the following model. As-deposited samples have a large number of EX centers and they contribute to the large n_2 . The EX center density decreases by annealing. This results in the decrease in n_2 when the annealing temperature is relatively low (600–700 °C). At around 800 °C, the signal from the P_b center appears and the density increases till ~ 900 °C. The large n_2 in this range is thus considered to arise mainly from P_b centers. Above this temperature, the defect density decreases rapidly. Around the temperature where the defect density decreases, Si nanocrystals start to grow. Probably the decrease in the surface-to-volume ratio by the formation and growth of nanocrystals results in the decrease in the defect density. The evidence of Si nanocrystals formation is obtained in Raman spectra. Figure 3(b) shows Raman spectra for the samples with 22 vol % excess Si. Below 900 °C, the spectra are amorphous-like, suggesting the existence of amorphous clusters.⁴⁴ A crystalline peak (520 cm^{-1}) starts to appear at 1000 °C and it becomes sharper at higher annealing temperatures. This evidences the growth of Si nanocrystals and is consistent with the decrease in the ESR signal intensity at the high annealing temperature range.

In the annealing temperature range where the growth of Si nanocrystals is confirmed, the annealing temperature dependence of the ESR signal intensity is different from that of n_2 [Figs. 2(a) and 2(c)]. For example, at 1250 °C, despite a very small defect density, the n_2 is relatively large. Moreover, despite almost the same defect density at 1250 °C for the samples with different excess Si concentrations, n_2 is larger for those with larger excess Si. These discrepancies suggest the existence of other origins for the large n_2 . We believe that in this annealing temperature range, quantized electronic states brought by quantum size effects are the major origin of large n_2 as have been predicted by some previous studies.^{3–6} In fact, in our previous work, we observed size-dependence of n_2 for the samples annealed at high

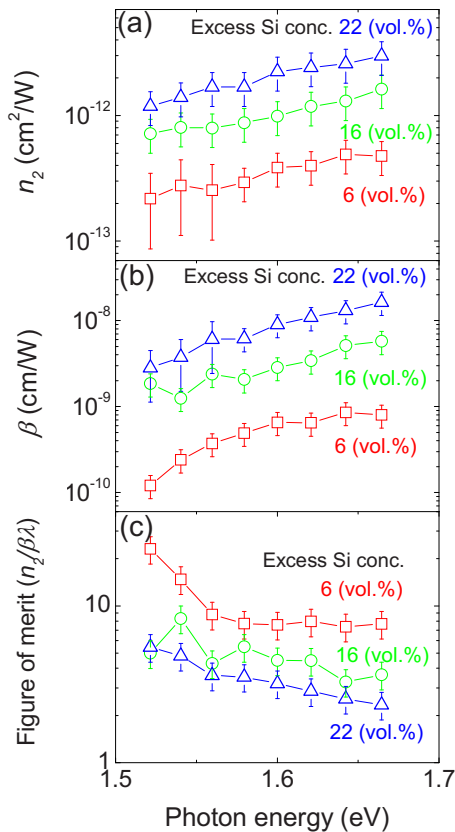


FIG. 5. (Color online) Photon energy dependence of (a) n_2 , (b) β , and (c) NFOM ($n_2/\beta\lambda$) for the samples with different excess Si concentrations (\square : 6, \circ : 16, \triangle : 22 vol %). The data of samples annealed at 1150 °C are shown.

temperatures.⁶ The experimental results agreed fairly well with a calculation which took into account quantized electronic states of Si nanocrystals.^{35,36}

C. Photon energy dependence of the nonlinear optical properties of SiO₂:Si-ncs

For optical switching and modulation applications of large n_2 , nonlinear figure of merit (NFOM), $n_2/\beta\lambda$, where λ is a wavelength, is proposed as one of the important parameters to deduce the device performance. Figures 5(a)–5(c) show the photon energy dependence of n_2 , β , and NFOM, respectively, for the samples annealed at 1150 °C. Although n_2 gradually decreases with decreasing the photon energy, NFOM increases because of the rapid decrease in β . Similar photon energy dependence is observed for the samples annealed at other temperatures.

Yıldırım and Bulutay^{35,36} calculated the real part of third order nonlinear susceptibility ($\text{Re } \chi^{(3)}$), which is proportional to n_2 , of Si nanocrystals doped SiO₂ by an atomic pseudo-potential approach. According to them, $\text{Re } \chi^{(3)}$ slightly decreases from 800 to 1550 nm. They also show that the NFOM drastically increases below the band gap energy of Si-ncs. Although our measurements are limited to the range from 1.52 to 1.66 eV, considering these reports and Fig. 5(c), SiO₂:Si-ncs are expected to show large NFOM at the com-

munication wavelength. In fact, Spano *et al.*⁵ reported that Si-ncs doped SiO₂N_y thin films have a large n_2 at 1550 nm ($\sim 5 \times 10^{-13}$ cm²/W).

IV. CONCLUSION

We performed comprehensive studies on third order nonlinear optical properties of SiO₂ films containing Si nanocrystals and/or nanoclusters by changing the annealing temperature and the excess Si concentration in wide ranges to reveal the origin of large n_2 and β . We demonstrated that n_2 and β exhibit complicated annealing temperature dependence. The detailed comparison of n_2 and ESR data revealed that defect states play a major role in the large n_2 when the annealing temperature is low, while their contributions become small when Si nanocrystals are grown in the films by high-temperature annealing. In the high-temperature annealing range, quantized electronic states of Si nanocrystals are considered to be the major origin of the large n_2 . Therefore, in SiO₂:Si-ncs systems, to maximize n_2 , the structure and the preparation parameters should be optimized by taking into account both the quantized electronic states and the defect states.

ACKNOWLEDGMENTS

This work was partly supported by the Research Grant in the Natural Science from Mitsubishi Foundation and by the Research Grant in Kawanishi-Shinmeiwa-Kinen Foundation.

- ¹S. Vijayalakshmi, H. Grebel, Z. Iqbal, and C. W. White, *J. Appl. Phys.* **84**, 6502 (1998).
- ²S. Vijayalakshmi, H. Grebel, G. Yaglioglu, R. Pino, R. Dorsinville, and C. W. White, *J. Appl. Phys.* **88**, 6418 (2000).
- ³G. Vijaya Prakash, M. Cazzanelli, Z. Gaburro, L. Pavesi, F. Iacona, G. Franzò, and F. Priolo, *J. Appl. Phys.* **91**, 4607 (2002).
- ⁴S. Hernández, P. Pellegrino, A. Martínez, Y. Lebour, B. Garrido, R. Spano, M. Cazzanelli, N. Daldosso, L. Pavesi, E. Jordana, and J. M. Fedeli, *J. Appl. Phys.* **103**, 064309 (2008).
- ⁵R. Spano, N. Daldosso, M. Cazzanelli, L. Ferraoli, L. Tartara, J. Yu, V. Degiorgio, E. Jordana, J. M. Fedeli, and L. Pavesi, *Opt. Express* **17**, 3941 (2009).
- ⁶K. Imakita, M. Ito, M. Fujii, and S. Hayashi, *J. Appl. Phys.* **105**, 093531 (2009).
- ⁷Y. Kanzawa, T. Kageyama, S. Takeoka, M. Fujii, S. Hayashi, and K. Yamamoto, *Solid State Commun.* **102**, 533 (1997).
- ⁸S. Takeoka, M. Fujii, and S. Hayashi, *Phys. Rev. B* **62**, 16820 (2000).
- ⁹F. Iacona, G. Franzò, and C. Spinella, *J. Appl. Phys.* **87**, 1295 (2000).
- ¹⁰S. Guha, B. Qadri, R. G. Musket, M. A. Wall, and T. Shimizu-Iwayama, *J. Appl. Phys.* **88**, 3954 (2000).
- ¹¹B. Jalali, *Phys. Status Solidi A* **205**, 213 (2008).
- ¹²Y. Kanemitsu, S. Okamoto, and A. Mito, *Phys. Rev. B* **52**, 10752 (1995).
- ¹³F. Z. Henari, K. Morgenstern, W. J. Blau, V. A. Karavanskii, and V. S. Dneprovskii, *Appl. Phys. Lett.* **67**, 323 (1995).
- ¹⁴S. Lettieri, O. Fiore, P. Maddalena, D. Ninno, G. D. Francia, and V. L. Ferrara, *Opt. Commun.* **168**, 383 (1999).
- ¹⁵S. Vijayalakshmi, M. A. George, and H. Grebel, *Appl. Phys. Lett.* **70**, 708 (1997).
- ¹⁶S. Vijayalakshmi, F. Shen, and H. Grebel, *Appl. Phys. Lett.* **71**, 3332 (1997).
- ¹⁷S. Vijayalakshmi, A. Lan, Z. Iqbal, and H. Grebel, *J. Appl. Phys.* **92**, 2490 (2002).
- ¹⁸E. Koudoumas, O. Kokkinaki, M. Konstantaki, N. Kornilios, S. Couris, S. Korovin, V. Pustovoi, and V. E. Oguzdin, *Opt. Mater.* **30**, 260 (2007).
- ¹⁹P. Cheng, H. Zhu, Y. Bai, Y. Zhang, T. He, and Y. Mo, *Opt. Commun.* **270**, 391 (2007).
- ²⁰S. Moon, A. Lin, B. H. Kim, P. R. Watekar, and W. T. Han, *J. Non-Cryst. Solids* **354**, 602 (2008).

- ²¹E. Borcella, M. Falconieri, S. Botti, S. Martelli, F. Bignoli, L. Costa, S. Grandi, L. Sangaletti, B. Allieri, and L. Depero, *Mater. Sci. Eng., B* **79**, 55 (2001).
- ²²C. Torres-Torres, A. López-Suárez, L. Tamayo-Rivera, R. Rangel-Rojo, A. Crespo-Sosa, J. C. Alonso, and A. Oliver, *Opt. Express* **16**, 18390 (2008).
- ²³A. López-Suárez, C. Torres-Torres, R. Rangel-Rojo, J. A. Royes-Esqueda, G. Santana, J. C. Alonso, A. Ortiz, and A. Oliver, *Opt. Express* **17**, 10056 (2009).
- ²⁴Q. Lin, J. Zhang, G. Piredda, R. W. Boyd, P. M. Fauchet, and G. P. Agrawal, *Appl. Phys. Lett.* **91**, 021111 (2007).
- ²⁵A. D. Bristow, N. Rotenberg, and H. M. van Driel, *Appl. Phys. Lett.* **90**, 191104 (2007).
- ²⁶M. Dinu, F. Quochi, and H. Garcia, *Appl. Phys. Lett.* **82**, 2954 (2003).
- ²⁷R. W. Boyd, *Nonlinear Optics* (Academic, San Diego, 2008), p. 212.
- ²⁸A. Maeda, M. Ono, H. Kishida, T. Manako, A. Sawa, M. Kawasaki, Y. Tokura, and H. Okamoto, *Phys. Rev. B* **70**, 125117 (2004).
- ²⁹A. Dowd, R. G. Elliman, M. Samoc, and B. Luther-Davies, *Appl. Phys. Lett.* **74**, 239 (1999).
- ³⁰L. Razzari, A. Gnoli, M. Righini, A. Dâna, and A. Aydinli, *Appl. Phys. Lett.* **88**, 181901 (2006).
- ³¹T. D. Krauss and F. W. Wise, *Appl. Phys. Lett.* **65**, 1739 (1994).
- ³²H. P. Li, B. Liu, C. H. Kam, Y. L. Lam, W. X. Que, L. M. Gan, C. H. Chew, and G. Q. Xu, *Opt. Mater.* **14**, 321 (2000).
- ³³S. Schmitt-Rink, D. A. B. Miller, and D. S. Chemla, *Phys. Rev. B* **35**, 8113 (1987).
- ³⁴L. Banyai, Y. Z. Hu, M. Lindberg, and S. W. Koch, *Phys. Rev. B* **38**, 8142 (1988).
- ³⁵H. Yildirim and C. Bulutay, *Phys. Rev. B* **78**, 115307 (2008).
- ³⁶H. Yildirim and C. Bulutay, *Opt. Commun.* **281**, 4118 (2008).
- ³⁷T. Takagahara and E. Hanamura, *Phys. Rev. Lett.* **56**, 2533 (1986).
- ³⁸F. Iacona, C. Bongiorno, C. Spinella, S. Boninelli, and F. Priolo, *J. Appl. Phys.* **95**, 3723 (2004).
- ³⁹M. Sheik-Bahae, A. A. Said, T. Wei, D. J. Hagan, and E. W. Van Stryland, *IEEE J. Quantum Electron.* **26**, 760 (1990).
- ⁴⁰K. Imakita, M. Ito, M. Fujii, and S. Hayashi, *Opt. Express* **17**, 7368 (2009).
- ⁴¹S. M. Prokes, W. E. Carlos, S. Veprek, and C. Ossadnik, *Phys. Rev. B* **58**, 15632 (1998).
- ⁴²A. Stesmans and F. Scheerlinck, *Phys. Rev. B* **51**, 4987 (1995).
- ⁴³M. Fujii, A. Mimura, S. Hayashi, K. Yamamoto, C. Urakawa, and H. Ohta, *J. Appl. Phys.* **87**, 1855 (2000).
- ⁴⁴N. Daldosso, G. Das, G. Dalba, S. Larcheri, R. Grisenti, G. Mariotto, L. Pavesi, F. Rocca, F. Priolo, G. Franzo, A. Irrera, M. Miritello, D. Pacifici, and F. Iacona, *Silicon Nanocrystal Nucleation as a Function of the Annealing Temperature in SiO_x Films*, MRS Symposia Proceedings No. 770 (Materials Research Society, Pittsburgh, 2003), p. 11.3.1.